Bone 138 (2020) 115511

Contents lists available at ScienceDirect

Bone

journal homepage: www.elsevier.com/locate/bone

Full Length Article

A cell-based combination product for the repair of large bone defects

Johan Lammens[a,b,*,1], Marina Maréchal[b,c,1], Hendrik Delport[b], Liesbet Geris[b,c,d,e], Hermann Oppermann[f], Slobodan Vukicevic[g], Frank P. Luyten[b,c]

[a] Department of Orthopaedic Surgery, University Hospitals Leuven, Herestraat 49, 3000 Leuven, Belgium
[b] Prometheus, Division of Skeletal Tissue Engineering of the KU Leuven, Herestraat 49, 3000 Leuven, Belgium
[c] Skeletal Biology and Engineering Research Center, KU Leuven, Herestraat 49, 3000 Leuven, Belgium
[d] Department of Mechanical Engineering, Biomechanics Section, KU Leuven, Celestijnenlaan 300, 3001 Heverlee (Leuven), Belgium
[e] Biomechanics Research Unit, GIGA In silico medicine, University of Liège, Quartier Hôpital, Avenue de l'Hôpital 1, 4000 Liège 1, Belgium
[f] Genera Research, Svetonedeljska cesta 2, 10436 Kalinovica, Sveta Nedelja, Croatia
[g] Laboratory for Mineralized Tissues, Center for Translational and Clinical Research, School of Medicine, University of Zagreb, Šalata ul. 2, 10000 Zagreb, Croatia

ARTICLE INFO

Keywords:
Large animal model
Bone Morphogenetic Protein
Periosteum-derived cells
Biologically exhausted defect

ABSTRACT

Regenerative cell-based implants using periosteum-derived stem cells were developed for the treatment of large 3 cm fresh and 4.5 centimeter biological compromised bone gaps in a tibial sheep model and compared with an acellular ceramic-collagen void filler. It was hypothesized that the latter is insufficient to heal large skeletal defects due to reduced endogenous biological potency.

To this purpose a comparison was made between the ceramic dicalciumphosphate scaffold (CopiOs®) as such, the same ceramic coated with clinical grade Bone Morphogenetic Protein 2 and 6 (BMP) only or a BMP coated cell-seeded combination product. These implants were evaluated in 2 sheep models, a fresh 3 cm critical size tibial defect and a 4.5 cm biologically exhausted tibial defect. For the groups in which growth factors were applied, BMP-6 was chosen at a dose of 344 μg for 3 cm and 1.500 μg or 3.800 μg for 4.5 cm defects. An additional group in the 4.5 cm defect was tested using BMP-2 in a dose of 1.500 μg. For all the cell based implants autologous periosteum-derived cells were used which were cultured in monolayer during 6 weeks. For the fresh defect 408 million cells and for the biologically exhausted tibial defect 612 million cells were drop-seeded on the BMP coated scaffolds. Bone healing was studied during 16 weeks postimplantation, using standard radiographs.

While fresh defects responded to all treatments, regardless the use of cells, the biologically hampered defects responded in half of the cases and only if the BMP-cell combination product was used, supporting the concept that cell-based therapies may become attractive in treating defects with a compromised biological status.

1. Introduction

The regeneration of bone to treat skeletal defects, due to trauma, infection or extensive tumor resections becomes challenging in case of severe bone loss. Therapies using allografts or synthetic bone void fillers are insufficient due to their limited and non-predictable biological potential [1,2]. In large defects, autografts, which are considered as "the gold standard" for non-union treatment, even in combination with Bone Morphogenetic Proteins (BMPs) do not convincingly alter the outcome due to the large volumetric dimensions necessary to bridge the gap and the insufficient bone stock of the human body [3,4]. So far, these difficult orthopedic problems are addressed with bone transport procedures or vascularized fibular grafts, but tissue engineered cell-based therapies now rising at the horizon may provide new opportunities for these challenging conditions [5–8].

Researchers put tremendous efforts in the development of cell-based Advanced Therapy Medicinal Products (ATMPs), but for the treatment of large bone defects they often cannot fulfil the surgeon's demand due to the mismatch between the small-scaled cell-based implants and the huge bone volumes to be repaired. Numerous biomaterial substitutes for bone defects have been reported, using different scaffolds, combinations of growth factors or use of cells but treatment efficiency remains uncertain because of unpredictable bone formation [9].

Moreover the regeneration of new bone is often not achieved due to the diseased microenvironment of the host inhibiting a correct interplay between implant and recipient [10].

* Corresponding author at: Department of Orthopaedic Surgery, University Hospitals Leuven, Herestraat 49, 3000 Leuven, Belgium.
E-mail address: johan.lammens@uzleuven.be (J. Lammens).
[1] These authors share first authorship.

https://doi.org/10.1016/j.bone.2020.115511
Received 29 February 2020; Received in revised form 14 June 2020; Accepted 14 June 2020
Available online 27 June 2020
8756-3282/

Previous work from our laboratory focused on the search for cell-based implants using periosteum-derived stem cells. It was documented that these cells preserve their multipotency despite extended culture expansion up to at least 30 population doublings [11]. The expanded periosteum-derived cells have unique properties and bone-forming capacities in comparison with mesenchymal stem cells from other sources [12]. Those cell-based implants showing a good biological potential, as demonstrated in an ectopic nude mouse model [13,14], were identified as good candidates for implantation in an orthotopic tibial mouse defect [13]. Following success in the nude mice, these implants were scaled up to larger dimensions and tested in a more clinically relevant animal model, i.e. large tibial bone defects of 3 and 4,5 cm in sheep, according to a previously published technique [15]. Sheep were divided in a group with a 3 cm fresh defect (FD group) or a 4.5 cm biologically exhausted defect (BED group) and treated with scaffold only, scaffold coated with BMP-2 or 6, and cell-based ATMPs with BMP-2 or 6. Throughout and after completion of the treatment, safety was carefully monitored. The aim of this study was to investigate to what extent the different implants could heal both types of bone defects.

2. Material and methods

2.1. Study design and surgery

All experiments in the sheep were performed with approval of the Ethical Committee of the Medanex Clinic (CRO, Diest, Belgium) and housed in accordance with the guidelines for the care of laboratory animals. The animal experiments were carried out in accordance with Directive 2010/63/EU and Belgian Royal Decree of 29 May 2013.

72 Swifter–Charollais female sheep were randomly assigned to a group in which a fresh 3 cm tibial defect was studied (FD), or a group with 4.5 cm defects that initially were left untreated to allow ingrowth of fibrotic scar tissue, reducing the biological repair capacity and designated as the biologically exhausted defects (BED).

For the FD group, 29 animals were divided in 3 subgroups, receiving scaffold only (n = 8), scaffold with BMP-6 (n = 8) or the cell-based ATMP (n = 13). For the BED group 43 animals were used, divided in 6 subgroups, i.e. scaffold only (n = 4), scaffold with BMP-2 (n = 8), scaffold with BMP-6 (n = 8), cell-based ATMP with BMP-2 (n = 7) and 2 groups of cell-based ATMP with different doses of BMP–6 (n = 8 for each group) (Table 1).

All surgical procedures were performed according to the Ilizarov technique, leading to mechanically well stabilized defects by means of a circular external fixator [15].

In the FD group the 3 cm fresh defect was created in the right tibia and a polymethyl-metacrylate spacer (PMMA) (Palacos®, Heraeus Medical, Wehrheim, Germany) was inserted immediately to induce a Masquelet membrane [16,17]. For the subgroup receiving the cell-based ATMP, a fragment of 1 by 2 cm of periosteum of the 3 cm resected tibial segment was sampled for expansion of the periosteum-derived cells (PDCs). Six weeks after the initial surgery the spacers were removed and the created biological chambers were filled with the implant according to each subgroup (Fig. 1). Sheep were then followed up for 16 weeks at which time point a definite analysis of the new bone regeneration was made using radiographs.

For the BED group 4.5 cm defects were created in the same way as the 3 cm defects in the FD group, but left untreated without insertion of a spacer. After 6 weeks, a complete debridement was performed of the fibrotic ingrowth. For the subgroup receiving the cell-based ATMP a simultaneous intervention was performed on the left tibia were through a small incision a fragment of 1 by 2 cm of periosteum was sampled for the cell culture of PDCs. Further treatment was analogous to the FD group with spacer insertion, i.e. exchange for the implant after 6 weeks according to the specific subgroups and follow-up till 16 weeks (Fig. 2).

2.2. Cell culture

The harvested periosteal samples measuring about 2 cm^2 were used for cell culture. The samples for cell culture were transported at 4 °C in high glucose Dulbecco's Modified Eagle Medium (DMEM, Life technologies Europe BV, Thermo Fisher Scientific, Merelbeke, Belgium) containing 2% antibiotic-antimycotic solution (AA) (100 units/ml penicillin, 100 µg/ml streptomycin and 025 µg/ml of amphotericin, Life technologies Europe BV, Thermo Fisher Scientific, Merelbeke, Belgium).

After drying and weighing, the specimens were rinsed twice with a Hank's Balanced Salt Solution (HBSS) not containing CaCl2 and MgCl2 (Life technologies Europe BV, Thermo Fisher Scientific, Merelbeke, Belgium), and minced in small pieces that were transferred to a 15 ml falcon tube containing a 0.2% collagenase solution in high glucose DMEM supplemented with 10% irradiated FBS (iFBS) and 1% antibiotics/antimycotic solution (=DMEM-c). Following an overnight incubation at 37 °C using slow rotation, the periosteum-derived cells were collected by centrifugation, washed twice and resuspended in high glucose DMEM-c. The cells were plated in a T75 flask and allowed to attach for 24 h. Non-adherent cells were removed by changing the medium.

For expansion, cells were cultured in monolayer in growth medium DMEM-c at 37 °C in a humidified atmosphere of 5% CO_2 in T175 flasks. The medium was refreshed every three days. When the cells reached 80 to 90% confluence, the cells were washed with HBBS and harvested by treatment with TrypLE (Life technologies Europe BV, Thermo Fisher Scientific, Merelbeke, Belgium). Cell passages were continued in the same way during six weeks. Six days before the assembly of the cell-based ATMP, the cells were seeded in T175 flasks without the antibiotic-antimycotic solution added to the medium. After two days of cell culture, potential bacterial contamination was excluded using culture bottles for detection of aerobic and anaerobic microorganism in the cell culture medium (BacT/ALERT® FA Plus Aerobic and BacT/ALERT® FN Plus Anaerobic – BioMerieux, Hospital Logistics, Aarschot, Belgium).

At cell harvest, residues of iFBS were removed using three washing steps with HBSS. The presence of Bovine Serum Albumin (BSA), residue of the iFBS, in the end product was checked using an ELISA kit (BCA Protein assay Kit) and the cells were resuspended in DMEM

Table 1
Different treatment groups in the fresh defect model and the biologically exhausted defect model.

Treatment group	Fresh defect (FD) of 3 cm	Biologically exhausted defect (BED) of 4.5 cm
	n = 29	n = 43
Scaffold only	8	4
Scaffold coated with BMP-6 (344 µg)	8	–
Scaffold coated with BMP-6 (1500 µg)	–	8
Scaffold coated with BMP-2 (1500 µg)	–	7
Cell-based ATMP with BMP-2 (1500 µg)	–	8
Cell-based ATMP with BMP-6 (344 µg)	13	–
Cell-based ATMP with BMP-6 (1500 µg)	–	8
Cell-based ATMP with BMP-6 (3800 µg)	–	8

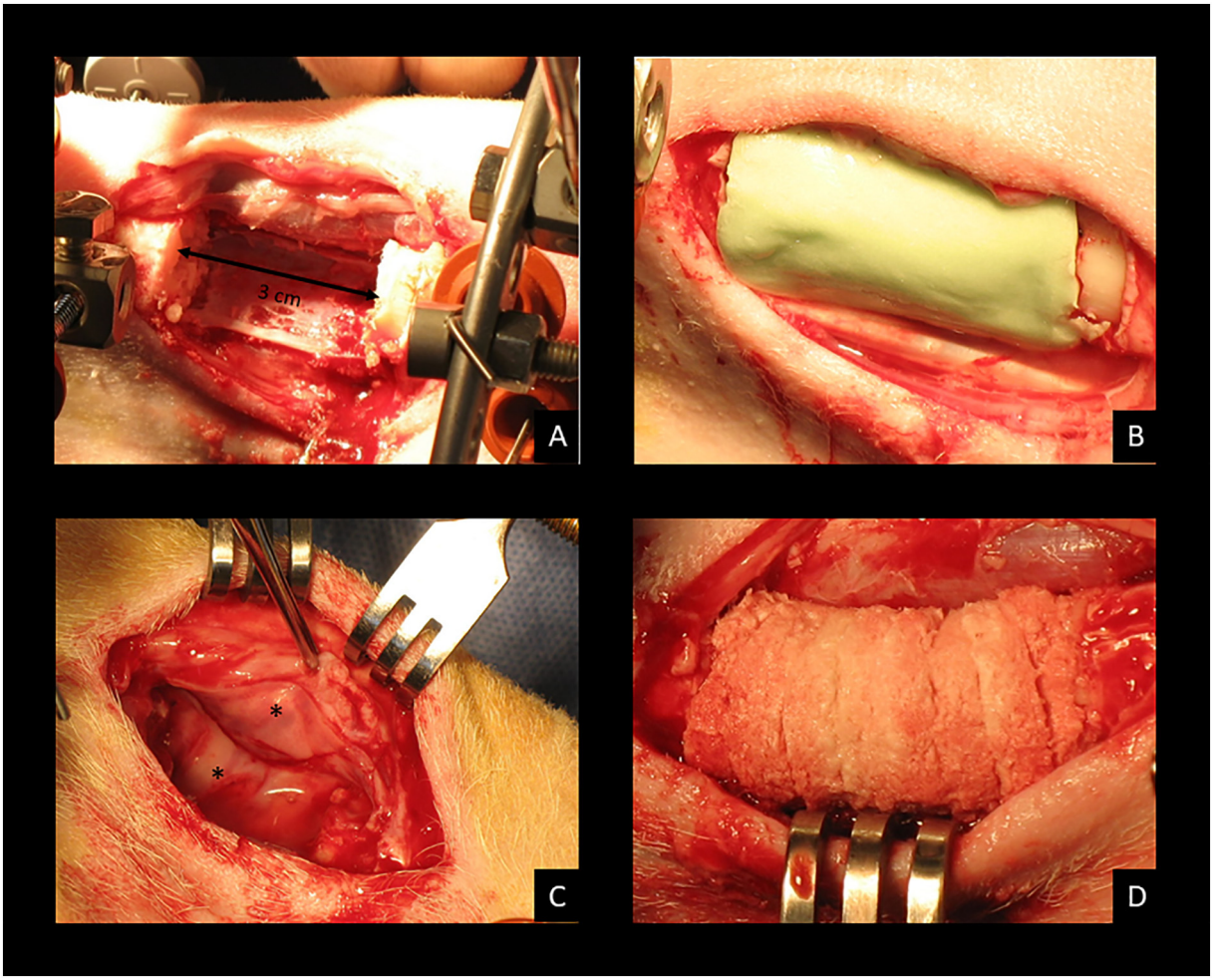

Fig. 1. Surgical intervention creating a Fresh Defect. 1st Surgery: A = fresh defect of 3 cm, B = implantation of PMMA spacer. 2nd Surgery: C = induced Masquelet membrane (*), D = implantation of ATMP.

supplemented with 10% autologous sheep serum.

2.3. Implants and ATMP assembly

For all the implants a dicalciumphosphate (DCP) scaffold CopiOs® (Zimmer, Warsaw, Indiana, USA) was used. From the original scaffold blocks, rings with a diameter of 2 cm and a central hole of 6 mm and a thickness of 4 mm were shaped. For the 3 cm FD group 8 rings were used, for the 4.5 cm BED group 12 rings.

For the combination of scaffold plus BMP, the rings were coated with either BMP-2 (Medtronic, Minneapolis, USA) or BMP-6 (Genera Inc., Kalinovica, Rakov Potok, Croatia) according to the subgroups.

For the FD group, the amount of BMP-6 coated onto each scaffold ring was 43 μg (total of 344 μg). For the BED group the amount of BMP-2 coated onto each scaffold ring was 125 μg (total of 1500 μg). For BMP-6125 μg and respectively 317 μg per ring was used for the two subgroups (total of 1500 μg and 3800 μg respectively). Subsequently, the scaffolds rings were incubated for 1 h at 37 °C and seeded with 51. 10^6 cells (total amount of cells 408 million for FD and 612 million for BED group) in 240 μl of DMEM with 10% autologous sheep serum and once again incubated for 1 h at 37 °C. At last 25 ml of DMEM with 10% autologous sheep serum was added for transport and implantation was performed within 3 h after assembly of the ATMP. The residual transport medium was centrifuged for calculating of cell seeding efficiency by counting the remaining cells.

2.4. Analysis of bone formation

To evaluate the new bone formation standard radiographs were taken in an anteroposterior and lateral direction at removal of the spacer and insertion of the implant (day 1) and after 3, 6, 12 and 16 weeks. For those animals showing good bone formation, further follow-up with radiographic imaging was performed up to 15 months.

These images were assessed for progression in bone formation and gap bridging through the use of a simple numerical score (Table 2, Fig. 3). If there was a total absence of bone formation, the score was zero. If callus progression was visible but without bridging the score was 1 and it increased according to the degree of cortical bridging up to 3 points when complete filling with full bridging was obtained. The numerical rating is described in Table 2 and Fig. 3 presents radiographic illustrations for each score.

Animals not obtaining a score equal or more than 2 were sacrificed at 16 weeks post-implantation and the bone specimens were analyzed by Nanofocus Computed Tomography (Nano CT, Phoenix NanoTom S, GE Measurement and Control Solutions, Germany) to study the spatial distribution and the remodeling of the newly formed bone tissue. The animals scoring 2 or more were kept alive for long term evaluation with radiographs and in vivo CT (CT Somatom Force, Siemens, Erlangen, Germany) evaluation at 5 months post-implantation and radiographs at 9–15 months postoperatively.

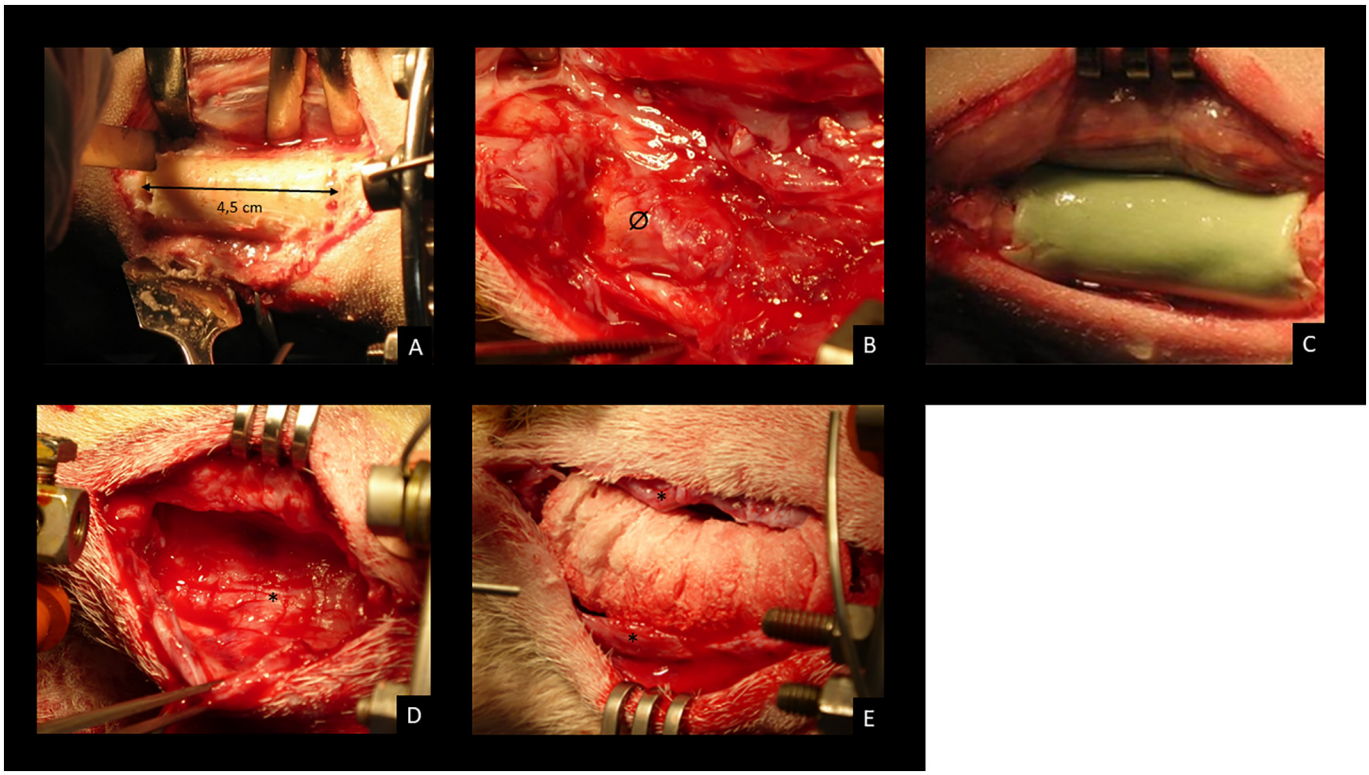

Fig. 2. Surgical intervention creating a biologically exhausted defect. 1st surgery: A = Defect of 4.5 cm, 2nd SURGERY: B = Fibrotic ingrowth (Ø), C = Implantation of PMMA spacer, 3rd surgery: D = Induced Masquelet membrane (*), E = Implantation of ATMP.

Table 2
The numerical rating on radiographs.

Score	Progression	Bridging
0	0	0
1	I	0
2	I	Partial
3	I	Full

2.5. Safety study

For safety evaluations, sacrificed animals underwent a sampling of the popliteal lymph nodes, liver, spleen and kidneys. The organs were embedded, sectioned and stained with haematoxilin and eosin to evaluate the organs for the presence of tumors, inflammation or infection. Blood samples were taken at different time points (at start of experiment as well as after 6, 12 and 16 weeks) and evaluated using reference data for sheep for total blood count, kidney function, liver function and alkaline phosphatase. On seven animals, a total necropsy was performed for macroscopic evaluation of all organs, followed by a

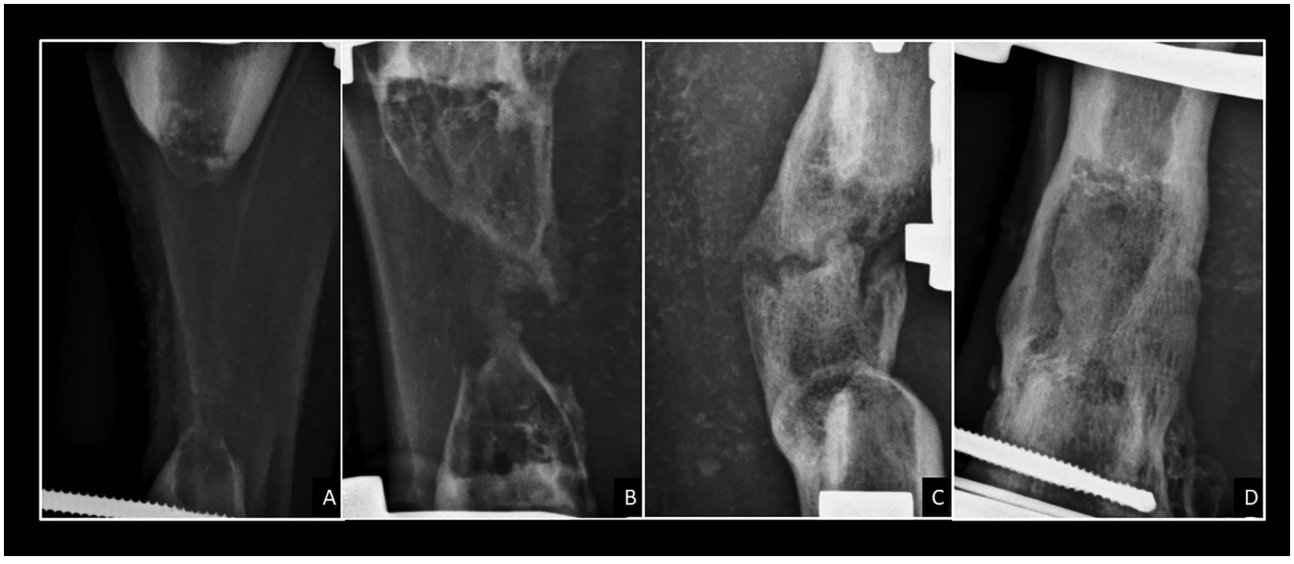

Fig. 3. Numerical rating on radiographs, A = score 0, B = score 1, C = score 2, D = score 3.

detailed histological examination.

2.6. Statistical analysis

A comparison of the outcomes in cell versus non cell treated groups was performed using the two-tailed Fisher's exact test with the significance level set at $p < 0.05$ (GraphPad Software, Inc., La Jolla, CA).

3. Results

3.1. Cell culture

The growth curves of the periosteum-derived cells from the animals included in the cell-based ATMP group showed a continuous proliferation with no signs of senescence using a Senescence-associated β-galactosidase assay (0 up to 0.3% cell senescence present) after 6 weeks of cell culture. The mean population doubling of the cells per passage was 2.6 during the cell culture period of 6 weeks. Screening tests throughout the period of cell culture showed absence of Mycoplasma and any other aerobic or anaerobic bacterial contamination. At harvest on day 41, a mean of $750 \cdot 10^6$ cells was available for each animal, of which $408 \cdot 10^6$ or $612 \cdot 10^6$ were seeded on the 3 respectively 4.5 cm dicalciumphosphate scaffold (DCP). The mean cell seeding efficiency was 86%.

3.2. Evaluation of bone formation

At day 1 after construct implantation, the contours of the DCP scaffold rings were slightly visible, but progressively disappeared during the following 6 weeks as seen on 3 and 6 weeks postoperative radiographs.

In the FD group, progression of the mineralization was observed in 21 of the 29 animals, obtaining score 2 at 6 or 12 weeks, while the other 8 did not show any bone formation. These 21 animals reached a score 3 at 16 weeks post-implantation, the distribution being 4 out of 8 control animals (CopiOs® only), 7 out of 8 treated with CopiOs® + BMP-6 (Fig. 4) and 10 out of 13 that received the ATMP cell-based implant (Table 3; Fig. 5).

In the BED group, only a limited number of animals showed progressive bone formation. The 4 controls treated with the DCP scaffold only, showed no signs of bone formation (score 0 in 4 out of 4). In those treated with the DCP scaffold plus BMP-6, 6 out of 8 defects remained empty or showed atrophic tapered bone outgrowth from both sides of the tibia (score 0). Two out of 8 animals showed some bone regeneration but with a residual central gap and no bridging (score 1). On the other hand the cell-based ATMPs (125 μg BMP-6/scaffold ring) resulted in 3 out of 8 completely bridged defects (score 3), 3 partial regenerations with a residual central gap (score 1) and 2 complete failures (score 0) (Fig. 6). Increasing the BMP 6 dose did not result in improved bone healing as the cell-based ATMPs (317 μg BMP-6/scaffold ring) only regenerated the defect in one animal whereas the 7 other animals remained completely empty (score 0). In the group of animals treated with a BMP-2 coated DCP scaffold (n = 7), 4 failures were recorded with no signs of bone regeneration (score 0) and 3 animals with some bone regeneration but still with a central gap (score 1). The sheep implanted with a BMP-2 coated ATMP seeded with cells (n = 8) had no bone regeneration in 4 out of the 8 animals whereas the other 4 showed a progressive filling and final bridging at 16 weeks (score 3) (Table 4; Fig. 7).

Although both BMP-2 and BMP-6 groups had a similar quantitative performance, the radiographic appearance of the newly formed callus was different. The BMP-2 animals had a 'suspension bridge' type of callus, initiating from the posterolateral side, probably due to intense interaction between host and implant (Fig. 8). In the BMP-6 treated animals the bone regeneration appeared in a uniform way throughout the implant as if recruiting predominantly cells from the ATMP, an observation that is subject for further investigation (Fig. 9).

All animals not reaching a score of 2 at 12 weeks, were sacrificed at 16 weeks post-implantation. Post-mortem Nano CT confirmed absent or inadequate bone formation. Animals with a score 2 or 3 at 16 weeks were kept alive. Healed tibiae from the non-sacrificed animals showed complete bone integration on radiographs and CAT-scan at 4 months post-implantation with clear signs of remodeling at 9–15 months since start of the treatment (Fig. 10).

3.3. Safety

During the experimental period no adverse events were observed. All sheep recovered uneventfully without local signs of infection at the wound site or abnormal swelling of the tibia. Biochemical parameters for kidney, liver function and blood cell count did not alter during the experimental period.

From sacrificed animals, the post-mortem samples of popliteal lymph nodes, spleen, liver and kidneys showed no histological abnormalities. In the 7 animals that underwent a total necropsy, no significant pathological changes were revealed.

3.4. Statistical analysis

The difference in outcome for cell versus non cell-based implants in the FD group was not significant at the $p < 0.05$ level ($p = 1.0$). Pooling these results of the BED animals, irrespective of the type of BMP used at optimal dose, demonstrates a significant difference between those treated with (n = 16) or without cells (n = 15), the success rate being 7 out of 16 versus 0 out of 15 ($p = 0.0068$).

4. Discussion

This study clearly documents that bone defects, deprived of a good biologic condition can still be regenerated by tissue engineered

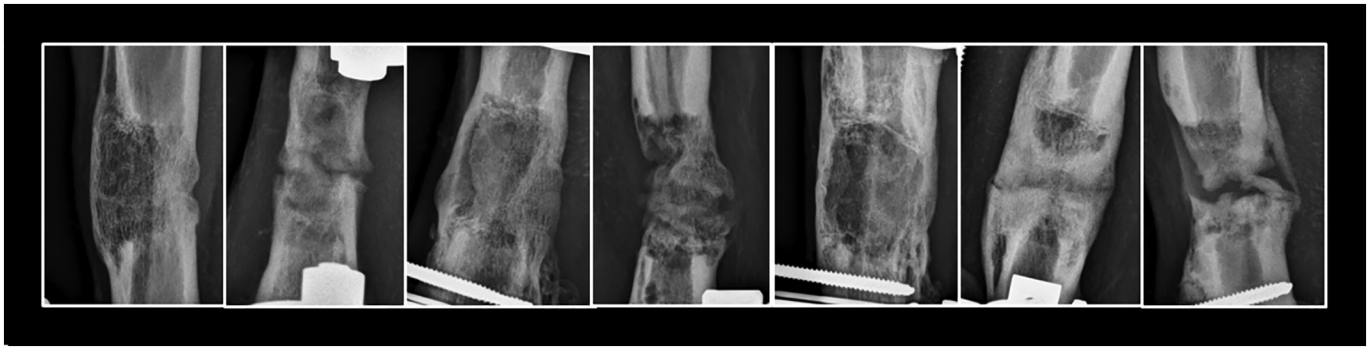

Fig. 4. Radiographs (score 2 or 3) at 16 weeks post-implantation. Group Fresh Defect with CopiOs® and BMP6 (344 μg) – n = 7.

Table 3
Numerical scoring on radiographs for the Fresh defect group.

Treatment group = Fresh Defects	n	Failure (score 0–1)	Success (score 2–3)
Scaffold only	8	4	4
Scaffold coated with BMP-6 (344 μg)	8	1	7
Cell-based ATMP and BMP-6 (344 μg)	13	3	10

constructs, to an extent that it becomes clinical relevant.

The comparison of fresh defects versus biologically exhausted defects in our study illustrates the difference in healing capacity of the different implants and reveals that neither the selected ceramic scaffold nor the same scaffold coated with BMP has sufficient potential to bridge a defect with a hampered biological status.

For this purpose we developed a cell-based combination product, in which the osteogenic periosteum-derived cells are cultured and seeded on a clinical grade BMP-2 or 6 coated calcium phosphate scaffold at a concentration of 47.000 cells per cubic millimeter, which is within the range of normal osteocyte densities as reported in the literature [18].

Taking too low amounts of cells may lead to a mathematical mismatch between the osteoprogenitor cell amount and the volumetric dimensions of the cavity to be filled. This can be considered as a result of 'Mother Nature's cellular paradox' i.e. the fact that cell size and architectural arrangements among cells, as known from histological analysis, are roughly the same for cell types with similar function across all mammalian species [19]. This simply means that cell size does not increase if body size increases and that for large volumes of bone repair in a (pre)clinical setting huge amounts of cells are required. This implies that ATMPs require a substantial upscaling effort to become successful for application in geometrically large defects as encountered in clinical practice. Although the cells for the assembly of the ATMP were currently cultured and seeded manually, future use of closed systems with robotics may become mandatory for application in the clinical setting.

The choice for periosteum-derived cells (PDCs) has been based on experimental work from our group, demonstrating their mesenchymal multipotency and bone forming capacity [11,20]. To be valid for use in patients the translational tests were performed with the dicalciumphosphate scaffold CopiOs®, being widely used in orthopedic surgery. In contrast to most ceramics, CopiOs® is a low calcium containing matrix with fast calcium release leading to quick disappearance on radiographs after 6 weeks post-implantation. Experiments using engineered implants with CopiOs® in an ectopic and orthotopic mouse model and calciumphosphate in an ectopic sheep model [13,] [21] were determinative for the choice of this scaffold. However, it is challenging to optimize the choice of scaffolds in large animal models, as this requires a lot of arms of the study and is not really justified in terms of the 3R principles for animal studies (refinement, reduction, replacement). There may indeed be room for improvement of the BMP delivery system as recently suggested [22–24]. Nevertheless in this study, an ELISA test for detecting BMP-6 in the transport medium of the implants could not reveal any residual protein, suggesting its high bond to the scaffold

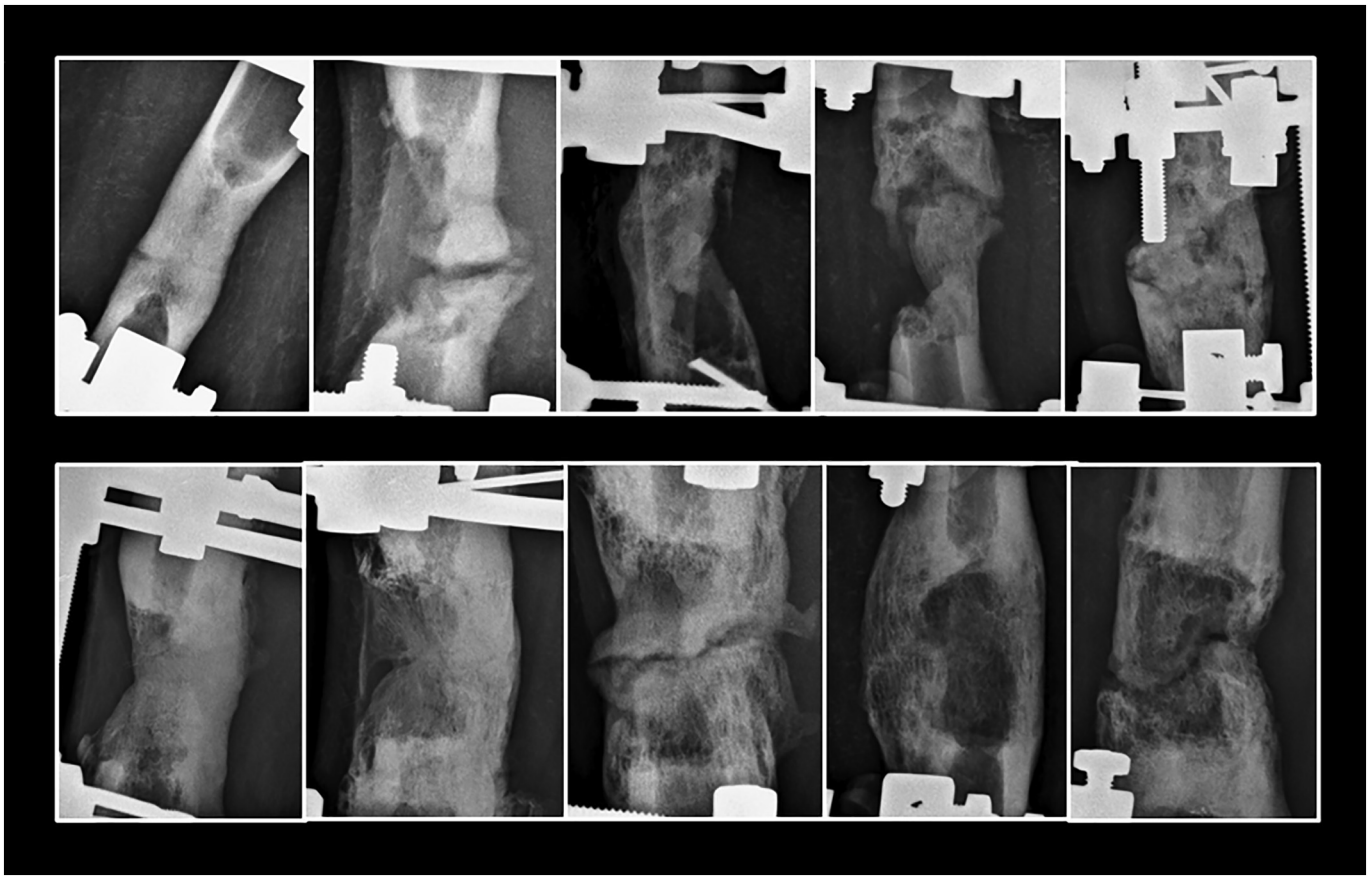

Fig. 5. Radiographs score 2 or 3) at 16 weeks post-implantation. Group Fresh Defect with CopiOs® and BMP6 (344 μg) and autologous periosteum-derived cells – n = 10.

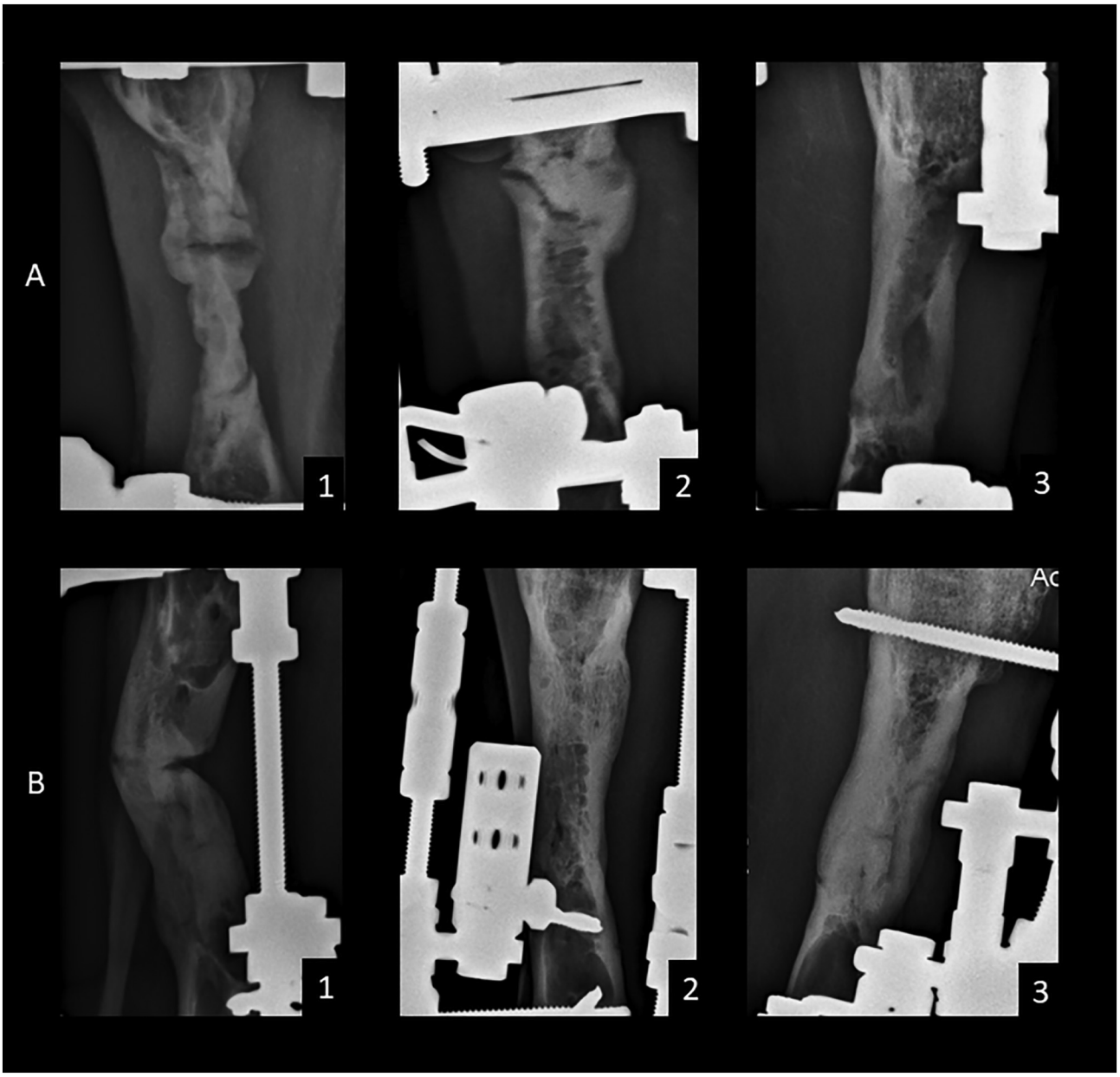

Fig. 6. Radiographs at 16 weeks post-implantation. Group Biologically Exhausted Defects – n = 3. A = CopiOs® and BMP6 (1500 μg) and autologous periosteum-derived cells 16 weeks post-implantation. B = CopiOs® and BMP6 (1500 μg) and autologous periosteum-derived cells 28 weeks post-implantation.

Table 4
Numerical scoring for the Biologically Exhausted Defect group.

Treatment group = Biologically Exhausted Defects	n =	Failure Score 0–1	Success Score 2–3
Scaffold only	4	4	0
Scaffold coated with BMP-6 (1500 μg)	8	8	0
Cell-based ATMP and BMP-6 (1500 μg)	8	5	3
Cell-based ATMP and BMP-6 (3800 μg)	8	7	1
Scaffold coated with BMP-2 (1500 μg)	7	7	0
Cell-based ATMP and BMP-2 (1500 μg)	8	4	4

(data not shown).

As growth factors we selected the novel designed clinical grade BMP-6 for both groups and for the BED group we also added a comparison with the bench mark BMP, being BMP-2 [25,26]. We identified BMP-2 and 6 as the best candidates for bone formation in an ectopic nude mouse study comparing BMP-2, 4, 6, 9 activity in cellular implants [27]. In the same study we noticed that bone formation was poor not only in BMP-4 and -9 cell-based implants but also in those without adding BMP. The effect of BMP-6 on in situ bone tissue engineering has also been sufficiently shown in a minipig model described by Bez et al. [28] and Mizrahi et al. [29] demonstrated that BMP-6 was even more efficient in bone formation than BMP-2 when overexpressed in mesenchymal stem cells. To avoid potential side effects, as reported for BMP-2 [30–32], a relatively low dose of the growth factors was used which nevertheless resulted in 4 out of 8 and 3 out of 8 healed animals for BMP-2 respectively BMP-6. Increasing the dose of BMP-6 did not improve the outcome and, surprisingly, even had an adverse effect as only one out of 8 animals showed relevant bone formation. This may appear contradictory to clinical recommendations of using higher doses and needs further research to examine dose related effects. According to the study of Nakamura [33] high concentrations of BMP-2 promotes bone resorption rather than bone formation. This was also demonstrated by Hunziker et al. [34] whose experiments using BMP-2 coated

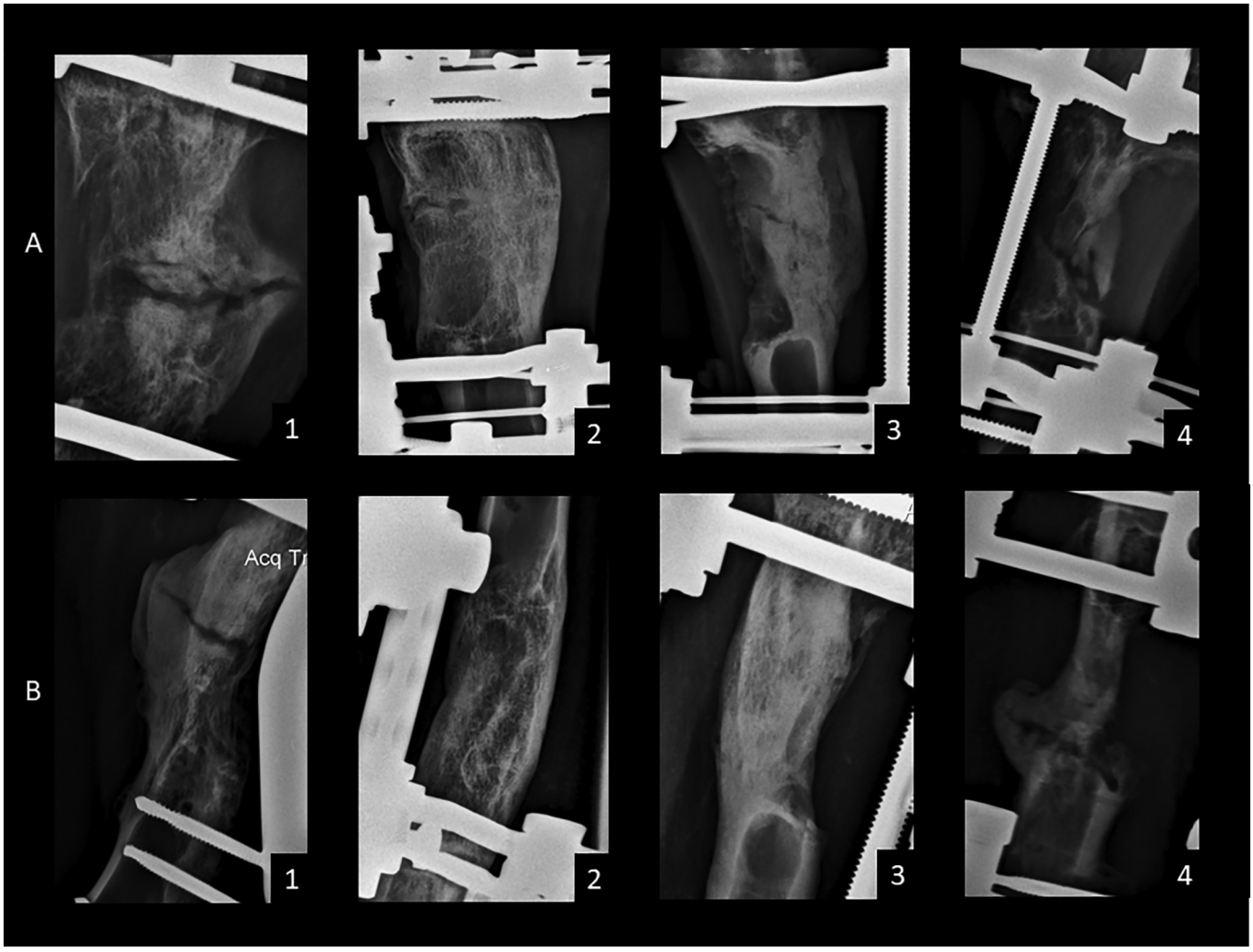

Fig. 7. Radiographs at 16 weeks post-implantation. Group Biologically Exhausted Defects – n = 4. A = CopiOs® and BMP2 (1500 μg) and autologous periosteum-derived cells 16 weeks post-implantation. B = CopiOs® and BMP2 (1500 μg) and autologous periosteum-derived cells 28 weeks post-implantation.

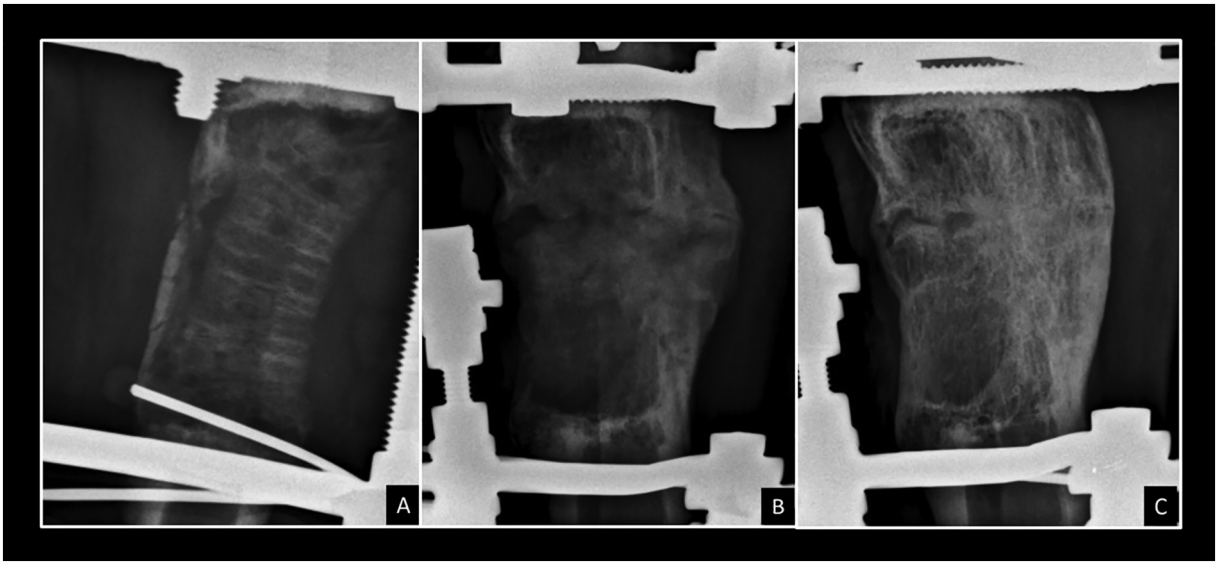

Fig. 8. Radiographs of ATMP (CopiOs® + BMP2 (1500 μg) + autologous periosteum-derived cells). A = at implantation, B = 6 weeks post-implantation, C = 16 weeks post-implantation.

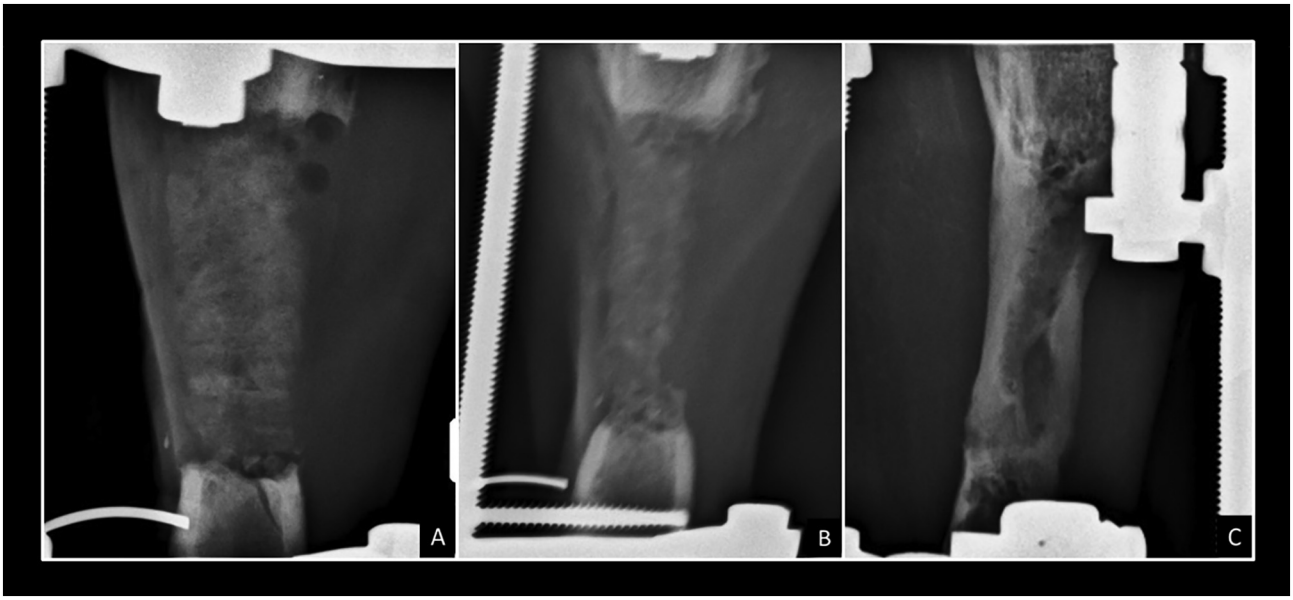

Fig. 9. Radiographs of ATMP (CopiOs® + BMP6 (1500 μg) + autologous periosteum-derived cells). A = at implantation, B = 6 weeks post-implantation, C = 16 weeks post-implantation.

implants were in favor of doses lower than 100 μg/g calcium phosphate coating material. The good effect of a low dose of BMP6 used in (pre) clinical studies [24,35,36], is possibly a consequence of its resistance to noggin and the affinity to all BMP-type 1 receptors [37].

The induced membrane technique of Masquelet [38,39] is recognized for providing a helpful addition to bone defect reconstruction nowadays and is widely used by orthopedic surgeons. Therefore, this technique was applied in our preclinical study. The method is based on the formation of an induced biological membrane around a PMMA spacer. It prevents fibrous tissue invasion in the bone defect and creates a pseudo-periosteal membrane rich in cells, vascularity and growth factors. It forms a biological chamber facilitating the ATMP implantation. We used scarification of the inner layer of the induced membrane as advocated by Luangphakdy et al. [40] at the time point of implantation. This induces bleeding from a healthy vascular bed without compromising the mechanical function of the outer layer. To promote integration of the implant with the host bone, the medullary canal at both bone ends close to the defect were opened to enhance blood supply providing nutrients and oxygen inside the implant. The implantation was performed 6 weeks after insertion of the spacer which is the optimal period as described in the literature [41]. At 6 weeks the membrane shows good vascularization and peak production of natural

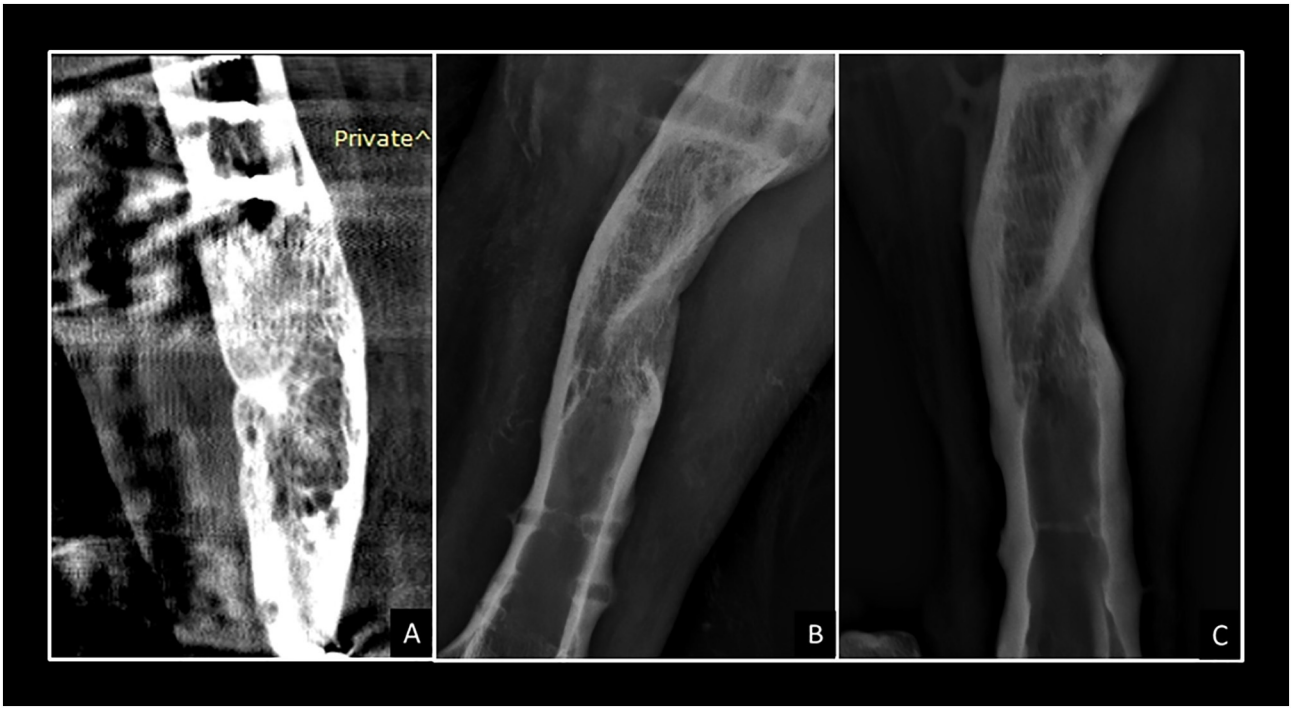

Fig. 10. Radiographs. A = in vivo CT scan after metal subtraction at 5 months post-implantation, B = radiograph at 9 months post-implantation, C = radiographs at 15 months post-implantation.

growth factors [42].

Bone healing was assessed radiographically by two independent experienced observers. When at 6 weeks post-implantation mineralization of the defect was observed, this always led to a progression of healing (score 2 or 3 at 16 weeks). Although some radiographic images might look delayed (score 2), they always evolved to score 3 allowing the removal of the fixator. For fresh defects the CopiOs® scaffold only showed a success in half of the cases, and enriched with BMP-6 the results improved to 7 out of 8 sheep. The cell-based ATMP, which is supposed to have the maximal biological potential, had possibly even a slightly lesser rate of healing (10 out of 13 animals), potentially due to normal biological variability. From these results we conclude that the treatment of fresh defects does not benefit from periosteum-derived cell supplementation. In contrast, BEDs, more representative for clinical situations, do not respond to scaffold-only or BMP-6 or -2 enriched scaffolds, all resulting in 0% healing. The cell-based ATMP with BMP-6 and BMP-2 in the same low dose (1500 μg) resulted in bone formation in respectively 3 out of 8 and 4 out of 8 of the cases. Therefore, adding cells to low dose BMP technology is a clinically relevant and significant improvement ($p = 0.0068$) of the therapy. Due to low numbers and limited power in this study computing exact probability is difficult. However an unbiased estimate can be obtained, using a Markov chain algorithm on the different groups in a $R \times C$ Exact Contingency table as described by Raymond and Rousset [43,44]. Comparing different treatment modalities (scaffold only, scaffold with BMP 1.5 mg, scaffold with BMP 1.5 mg plus cells) within the biological exhausted defects reveals a significant difference for those treated with cells ($p = 0.0046$) versus the scaffold only or scaffold + BMP.

This success rate does not yet exceed 50% but given the size and poor biological condition of the studied defects, these results already show that cell-based ATMPs have the potential to bridge this kind of large bone defects. Several improvements are possible and could be addressed in further studies. They include, but are not limited to, further optimization of scaffold technology, methods to increase survival of the implanted cells [45,46], priming and selecting the cells before implantation as suggested by Bolander et al. [13,47], the further optimization of dosing of cells and growth factors [48,49], and a more sophisticated immobilization device allowing for progressive load application leading to enhanced tissue integration [50].

It has to be noticed that bone formation in defect reconstruction requires special attention as there is a difference between the amount of newly formed bone and the structural integrity necessary for the mechanical loading of a bone allowing unprotected weight bearing. It needs to be emphasized that the scientist's interest in the bone forming capacity of an implant does not always match the clinician's need for a functionally repaired bone. Visible bone growth throughout a bone defect may indicate that the implant has an osteogenic potential but does not imply that it is clinically relevant [51].

Animal studies often report good results in so-called critical size bone defects, but this should be interpreted with utmost care as the described models use freshly created defects, which is in contrast with the real clinical situation. In these fresh defects the biological repair capacity can be surprisingly high due to the interaction of the implant and the host. In a clinical setting, scarring, poor vascularization and destroyed soft tissues/periosteum compromise the biological response. In such a setting, the regeneration process relies more on the intrinsic bone forming potency of the implant [52,53].

To our knowledge no reports on cell-based therapies have shown the ability to bridge such large biologically exhausted defects in a more robust way. We consider this study as the first to demonstrate the capacity of restoring large bone volumes in conditions that simulate the real clinical situation.

No analysis based on histology, micro CT or biomechanical testing has been made and is a limitation of our study but to overcome this, the animals with good bone bridging (score 2–3) were not sacrificed but considered as fully healed. During a period of approximately three years, in which they were bearing full weight, no adverse events occurred which confirms the good biomechanical properties of the restored bone.

Another unresolved issue is the lack of knowledge about the mechanism of the in vivo release of the BMPs from the scaffold which might be responsible for the variations in outcome in the study. Therefore, smart scaffolds with controlled BMP release could be part of future developments as well as further improvements by designing bone implants that don't rely on BMP technology. The developmental engineering principles, such as the use of ATMPs composed of organoid bioassembles which is currently under study [54], may move the field from combination products to engineered living tissues.

CRediT authorship contribution statement

Johan Lammens: Conceptualization, Methodology, Validation, Formal analysis, Investigation, Writing - original draft, Visualization, Funding acquisition. **Marina Maréchal:** Conceptualization, Methodology, Validation, Investigation, Resources, Writing - review & editing, Project administration. **Hendrik Delport:** Conceptualization, Methodology, Validation, Investigation, Writing - original draft. **Liesbet Geris:** Conceptualization, Methodology, Validation, Formal analysis, Resources, Investigation, Writing - review & editing, Visualization, Supervision, Funding acquisition. **Hermann Oppermann:** Resources. **Slobodan Vukicevic:** Validation, Resources, Writing - review & editing. **Frank P. Luyten:** Conceptualization, Methodology, Validation, Resources, Writing - review & editing, Visualization, Supervision, Funding acquisition.

Declaration of competing interest

None.

Acknowledgments

We are grateful for the excellent assistance of the highly skilled lab tech team of Prometheus and for the professional help of Lieve Ginckels during the surgical procedures.

This research was supported by grants from IWT-TBM (Flanders Belgium – Project number 110702), EIT Health (supported by the EIT, a body of the European Union), C3 (internal funding, KU Leuven, Belgium), Bone4kids (universiteitsfonds KU Leuven) and Hercules Foundation (project AKUL 13/47). This study was generated at Prometheus, the Division of Skeletal Tissue Engineering of the KU Leuven (www.kuleuven.be/prometheus).

References

[1] P.T. Ogink, F.R. Teunissen, J.R. Massier, K.A. Raskin, J.H. Schwab, S.A. Lozano-Calderon, Allograft reconstruction of the humerus: complications and revision surgery, J. Surg. Oncol. 119 (3) (2019) 329–335.
[2] H.S. Sohn, J.K. Oh, Review of bone graft and bone substitutes with an emphasis on fracture surgeries, Biomater Res 23 (2019) 9.
[3] T.H. Tosounidis, P.V. Giannoudis, Biological facet of segmental bone loss reconstruction, J. Orthop. Trauma 31 (Suppl. 5) (2017) S27–S31.
[4] C. Mauffrey, B.T. Barlow, W. Smith, Management of segmental bone defects, J Am Acad Orthop Surg 23 (2015) 143–153.
[5] A. Trounson, R.G. Thakar, G. Lomax, D. Gibbon, Clinical trials for stem cell therapies, BMC Med. 9 (2011) 52.
[6] E. Lopez-Ruiz, G. Jiménez, A. de Cienfuegos, C. Antich, R. Sabata, J.A. Marchal, P. Galvez-Martin, Advances of hyaluronic acid in stem cell therapy and tissue engineering, including current clinical trials, Eur Cell Mater 37 (2019) 186–213.
[7] A. Ho-Shui-Ling, J. Bolander, L.E. Rustom, A.W. Johnson, F.P. Luyten, C. Picart, Bone regeneration strategies: engineered scaffolds, bioactive molecules and stem cells current stage and future perspectives, Biomaterials. 180 (2018) 143–162.
[8] S. Palombella, S. Lopa, S. Gianola, L. Zagra, M. Moretti, A.B. Lovati, Bone marrow-derived cell therapies to heal long-bone nonunions: a systemic review and meta-analysis - which is the best available treatment, Stem Cells Int (2019 Dec 27) 3715964, , https://doi.org/10.1155/2019/3715964. eCollection 2019.
[9] W. Wang, K.W.K. Yeung, Bone grafts and biomaterials substitutes for bone defect repair: a review, Bioact Mater 2 (4) (2017) 224–247.

[10] B.D. Sui, C.H. Hu, A.Q. Liu, C.X. Zheng, K. Xuan, Y. Jin, Stem cell-based bone regeneration in diseased microenvironments: challenges and solutions, Biomaterials 196 (2019) 18–30.

[11] C. De Bari, F. Dell'Accio, J. Vanlauwe, J. Eyckmans, I.L. Khan, C.W. Archer, E.A. Jones, D. McGonagle, T.A. Mitsiadis, C. Pitzalis, F.P. Luyten, Mesenchymal multipotency of adult human periosteal cells demonstrated by single-cell lineage analysis, Arthritis Rheumatism 54 (4) (2006) 1209–1221.

[12] S. Roberts, N. van Gastel, G. Carmeliet, F.P. Luyten, Uncovering the periosteum for skeletal regeneration: the stem cell that lies beneath, Bone 70 (2015) 10–18.

[13] J. Bolander, W. Ji, J. Leijten, L. Moreira Teixeira, V. Bloemen, D. Lambrechts, M. Chaklade, F.P. Luyten, Healing of a large long-bone defect through serum-free in vitro priming of human periosteum-derived cells, Stem Cell Reports 8 (2017) 758–772.

[14] S.J. Roberts, L. Geris, G. Kerckhofs, E. Desmet, J. Schrooten, F.P. Luyten, The combined bone forming capacity of human periosteal derived cells and calcium phosphates, Biomaterials 32 (2011) 4393–4405.

[15] J. Lammens, M. Maréchal, L. Geris, J. Van der Aa, H. Van Hauwermeiren, F.P. Luyten, H. Delport, Warning about the use of critical-size defects for the translational study of bone repair: analysis of a sheep tibial model, Tissue Eng Part C Methods 23 (11) (2017) 694–699.

[16] A.C. Masquelet, T. Begue, The concept of induced membrane for reconstruction of long bone defects, Orthop. Clin. N. Am. 41 (2010) 27–37.

[17] V. Viateau, G. Guillemin, Y. Calando, D. Logeart, K. Oudina, L. Sedel, D. Hannouche, V. Bousson, H. Petite, Induction of a barrier membrane to facilitate reconstruction of massive segmental diaphyseal bone defects: an ovine model, Vet. Surg. 35 (2006) 445–452.

[18] B.S. Noble, The osteocyte lineage, Arch. Biochem. Biophys. 473 (2008) 106–111.

[19] LT. Threadgold, The Ultrastructure of the Animal Cell. second edition. Pergamom Press Limited, Oxford, England, 1967, pp. 32–39 (ISBN 0-08-018-957-1).

[20] J. Eyckmans, S.J. Roberts, J. Schrooten, F.P. Luyten, Clinical relevant model of osteoinduction: a process requiring calcium phosphate and BMP/Wnt signaling, J. Cell. Mol. Med. 14 (6B) (2010) 1845–1856.

[21] Damien Le Nihouannen, Guy Daculsi, Afchine Saffarzadeh, Olivier Gauthier, Séverine Delplace, Paul Pilet, Pierre Layrolle, Ectopic Bone Formation by Microporous Calcium Phosphate Ceramic Particles in Sheep Muscles, Bone 36 (6) (2005) 1086–1093 10,1016.

[22] W. Ji, G. Kerckhofs, C. Geeroms, M. Marechal, L. Geris, F.P. Luyten, Deciphering the combined effect of bone morphogenetic protein 6 and calcium phosphate on bone formation capacity of periosteum derived cells-based tissue engineering constructs, Acta Biomater. 80 (2018 Oct 15) 97–107.

[23] S. Vukicevic, Pecina M. Stokovic, Is ceramics an appropriate bone morphogenetic protein delivery system for clinical use? Int. Orthop. 43 (2019) 1275–1276.

[24] L. Grgurevic, H. Opperman, M. Pecin, I. Erjavec, H. Capak, M. Paul, S. Karlovic, V. Kufner, M. Lipar, J.B. Spoljar, T. Bordukalo-Niksic, D. Maticic, M. Peric, R. Windhager, T.K. Sampath, S. Vukicevic, Recombinant Human Bone Morphogenetic Protein 6 delivered within autologous blood clot coagulum restores critical size segmental defects of ulna in rabbits, JBMR Plus 3 (5) (2019) e10085.

[25] S. Vukicevic, L. Grgurevic, BMP-6 and mesenchymal stem cell differentiation, Cytokine Growth Factor Rev. 20 (2009) 441–448.

[26] S. Vukicevic, H. Oppermann, D. Verbanac, M. Jankolija, I. Popek, J. Curak, J. Brkljacic, M. Pauk, I. Erjavec, I. Francetic, I. Dumic-Cule, M. Jelic, D. Durdevic, T. Vlahovic, R. Novak, V. Kufner, T.B. Niksic, M. Kozlovic, Z.B. Tomisic, J. Bubic-Splojar, I. Bastalic, S. Vikic-Topic, M. Peric, M. Pecina, L. Grgurevic, The clinical use of bone morphogenetic proteins revisited: a novel biocompatible carrier device OSTEOGROW for bone healing, Int. Orthop. 38 (2014) 635–647.

[27] J. Bolander, W. Ji, L. Geris, V. Bloemen, Y.C. Chai, J. Schrooten, F.P. Luyten, The combined mechanism of bone morphogenetic protein- and calcium phosphate-induced skeletal tissue formation by human periosteum derived cells, Eur Cells Mater 31 (2016) 11–25.

[28] M. Bez, D. Sheyn, W. Tawackoli, P. Avalos, G. Shapiro, J.C. Giaconi, X. Da, S.B. David, J. Gavrity, H.A. Awad, H.W. Bae, E.J. Ley, T.J. Kremen, Z. Gazit, K.W. Ferrara, G. Pelled, D. Gazit, In situ bone tissue engineering via ultrasound-mediated gene delivery to endogenous progenitor cells in mini-pigs, Sci Transl Med. 9 (390) (2017) eaal3128.

[29] O. Mizrahi, D. Sheyn, W. Tawackoli, I. Kallai, A. Oh, S. Su, X. Da, P. Zarrini, G. Cook-Wiens, D. Gazit, Z. Gazit, BMP-6 is more efficient in bone formation than BMP2 when overexpressed in mesenchymal stem cells, Gene Ther. 20 (2013) 370–377.

[30] M.C. Simmonds, J.V.E. Brown, M.K. Heirs, J.P.T. Higgins, R.J. Mannion, M.A. Rodgers, L.A. Stewart, Safety and effectiveness of recombinant human bone morphogenetic protein-2 for spinal fusion. A meta-analysis of individual-participant data, Ann. Intern. Med. 158 (2013) 877–889.

[31] R. Fu, S. Selph, M. McDonagh, K. Peterson, A. Tiwari, R. Chou, M. Helfand, Effectiveness and harms of recombinant human bone morphogenetic protein-2 in spine fusion. A systemic review and meta-analysis, Ann. Intern. Med. 157 (2013) 890–902.

[32] Woo, et al., Adverse events after recombinant human BMP2 in nonspinal orthopaedic procedures, Clin. Orthop. Relat. Res. 471 (2013) 1707–1711.

[33] M. Nakamura, Y. Nakamichi, H. Nakamura, Udagawa, Osteoclastogenesis and bone resorption, Nihon Rinsho. Japanese J Clin Med 67 (5) (2009) 889–896.

[34] E.B. Hunziker, J. Jovanovic, A. Horner, M.J.B. Keel, K. Lippuner, N. Shintani, Optimisation of BMP-2 dosage for the osseointegration of porous titanium implants in an ovine model, Eur Cells Mater 32 (2016) 241–256.

[35] S. Vukicevic, L. Grgurevic, I. Erjavec, M. Pecin, T. Bordukalo-Niksic, N. Stokovic, M. Lipar, H. Capak, D. Maticic, R. Windhager, T.K. Sampath, M. Gupta, Autologous blood coagulum is a physiological carrier for BMP6 to induce new bone formation and promote posterolateral lumbar spine fusion in rabbits, J. Tissue Eng. Regen. Med. 14 (2020) 147–159.

[36] C. Chiari, L. Grgurevic, T. Bordukalo-Niksic, H. Oppermann, A. Valentinitsch, Recombinant human BMP6 applied within Autologous Blood Coagulum accelerates bone healing: Randomized controlled trial in High Tibial Osteotomy patients, J Bone Miner Res (June 2020), https://doi.org/10.1016/j.bone.2005.02.017.

[37] L. Grgurevic, I. Erjavec, I. Dumic-Cule, T. Bordukalo-Niksic, M. Pauk, V. Trkulja, D. Maticic, M. Pecin, M. Lipar, M. Peric, S. Vukicevic, Osteogrow: a novel bone graft substitute for orthopedic reconstruction, in: S. Vukicevic, T.K. Sampath (Eds.), Bone Morphogenetic Proteins: Systems Biology Regulators, PIR Series, Springer International Publishing, 2017, pp. 215–228.

[38] J.C. Aurégan, T. Begue, Induced membrane for treatment of critical sized bone defect: a review of experimental and clinical experiences, Int. Orthop. 38 (9) (2014) 1971–1978.

[39] A. Masquelet, N.K. Kanakaris, L. Obert, P. Stafford, P.V. Giannoudis, Bone repair using the Masquelet technique, J. Bone Joint Surg. Am. 101 (11) (2019) 1024–1036.

[40] V. Luangphakdy, G.E. Pluhar, N.S. Piuzzi, J.C. D'Alleyrand, C.S. Carlson, J.E. Bechtold, J. Forsberg, G.F. Muschler, The effect of surgical technique and spacer texture on bone regeneration: a caprine study using the Masquelet technique, Clin Orthop Rel Res 475 (10) (2017) 2575–2585.

[41] P.V. Giannoudis, O. Faour, T. Goff, N. Kanakaris, R. Dimitriou, Masquelet technique for the treatment of bone defects: tips-tricks and future directions, Injury 42 (2011) 591–598.

[42] O.-M. Aho, P. Lehenkari, J. Ristiniemi, S. Lehtonen, J. Risteli, H.-V. Leskelä, The mechanism of action of induced membranes in bone repair, J. Bone Joint Surg. 95 (2013) 597–604.

[43] http://www.physics.csbsju.edu/stats/exact.

[44] M. Raymond, F. Rousset, An exact test for population differentiation, Evolution 49 (6) (1995) 1280–1283.

[45] S. Stegen, G. Carmeliet, Hypoxia, hypoxia-inducible transcription factors and oxygen-sensing prolyl hydroxylases in bone development and homeostasis, Curr. Opin. Nephrol. Hypertens. 28 (2019) 328–335.

[46] P.J. Stiers, S. Stegen, N. van Gastel, R. Van Looveren, S. Torrekens, G. Carmeliet, Inhibition of the oxygen sensor PHD2 enhances tissue-engineered endochondral bone formation, JBMR 34 (2019) 333–348.

[47] J. Bolander, T. Herpelinck, M. Chaklader, C. Gklava, L. Geris, F.P. Luyten, Single-cell characterization and metabolic profiling of in vitro cultured human skeletal progenitors with enhanced in vivo bone forming capacity, Stem Cells Transl. Med. 9 (3) (2020) 389–402.

[48] C.P. Hofstetter, A.S. Hofer, A.D. Levi, Exploratory meta-analysis on dose-related efficacy and morbidity of bone morphogenetic protein in spinal arthrodesis surgery, J Neurosurg Spine 24 (2016) 457–475.

[49] M. Bouyer, R. Guillot, J. Lavaud, C. Plettinx, C. Olivier, V. Curry, J. Boutonnat, J.L. Coll, F. Peyrin, V. Josserand, G. Bettega, C. Picart, Surface delivery of tunable doses of BMP-2 from an adaptable polymeric scaffold induces volumetric bone regeneration, Biomaterials 104 (2016) 168–181.

[50] S. Herberg, A.M. McDermott, P.N. Dang, D.S. Alt, R. Tang, J.H. Dawahare, D. Varghai, J.Y. Shin, A. McMillan, A.D. Dikina, F. He, Y.B. Lee, Y. Cheng, K. Umemori, P.C. Wong, H. Park, J.D. Boerckel, E. Alsberg, Combinatorial morphogenetic and mechanical cues to mimic bone development for defect repair, Sci Adv 5 (8) (2019) eaax2476.

[51] P. Niemeyer, T.S. Schönberger, J. Hahn, P. Kasten, J. Fellenberg, N. Suedkamp, A.T. Mehlhorn, S. Milz, S. Pearce, Xenogenic transplantation of human mesenchymal stem cells in a critical size defect of the sheep tibia, Tissue Eng Part A 16 (2010) 33–43.

[52] J.A. Bishop, A.A. Palanca, M.J. Bellino, D.W. Lowenberg, Assessment of compromised fracture healing, J Am Acad Orthop Surg 20 (2012) 273–282.

[53] C.C. Lin, S.C. Lin, C.C. Chiang, M.C. Chang, O.K. Lee, Reconstruction of bone defect combined with massive loss of periosteum using injectable human mesenchymal stem cells in biocompatible ceramic scaffolds in a porcine animal model, Stem Cells Int 2019 (2019 Nov 23) 6832952, , https://doi.org/10.1155/2019/6832952. eCollection 2019.

[54] G. Nilsson Hall, L.F. Mendes, C. Gklava, L. Geris, F.P. Luyten, I. Papantoniou, Developmentally engineered callus organoid bioassemblies exhibit predictive in vivo bone healing, Advanced Science 7 (2) (2019 Dec 10) 1902295, , https://doi.org/10.1002/advs.201902295 eCollection 2020 Jan.